Structure and diffracted intensity in a model for irreversible island-forming chemisorption with domain boundaries

J. W. Evans and R. S. Nord
Ames Laboratory and Department of Chemistry, Iowa State University, Ames, Iowa 50011

(Received 8 September 1986; accepted 20 October 1986)

Despite the awareness that island-forming chemisorption is often kinetically limited and intrinsically nonequilibrium, there is little sophisticated analysis of the corresponding island structure or diffracted intensity. Here we analyze a model where species irreversibly and immobilely chemisorb (commensurately) from a precursor source, with distinct rates for island nucleation (chemisorption in an empty region) and growth (chemisorption at island perimeters), the latter rates being larger. Specifically, we consider the formation of one-dimensional double-spaced islands, and two-dimensional checkerboard C(2×2) islands on a square lattice. In both cases (permanent) domain boundaries form between out-of-phase islands. We analyze scaling of the saturation coverage, a characteristic linear island dimension, spatial correlations, etc., with the ratio of growth to nucleation rates. The structure of individual islands, and of the saturation domain boundary "network" are elucidated. The corresponding diffracted intensity exhibits significant interference at superlattice beams, and diminution at integral order beams as saturation is approached.

I. INTRODUCTION

We consider simple (but mathematically nontrivial) models wherein species *irreversibly and immobilely* (commensurately) *chemisorb* (from a physisorbed precursor "source"), with distinct rates for island nucleation, growth, and possibly coalescence. These rates include a common (possibly) time-dependent factor, corresponding to the (spatial) average precursor source density. This factor does not affect the chemisorbed adlayer statistics, at any specified coverage, but only modulates the time scale (and is suppressed here). Although mobility and desorption are neglected in the chemisorbed state, producing nonequilibrium island distributions,[1] these mechanisms are assumed to be operative in equilibrating the physisorbed precursor (at a rate much faster than chemisorption).

The cooperativity manifested by configuration dependent chemisorption rates could be associated with (i) source density variations which behave like $e^{-\beta J(\mathbf{r})}$ for an equilibrated, low-density, ideal gas precursor [where $J(\mathbf{r})$ is the binding energy at site $\mathbf{r}$, incorporating interactions with nearby chemisorbed species]; thus the density is enhanced by attractive interactions near island edges (cf. Ref. 2 which assumes nonactivated chemisorption at a rate proportional to this density); (ii) activated chemisorption, where the activation energy barrier is modified by physisorbed–chemisorbed species interactions; the barrier is lowered, again enhancing chemisorption, near island edges (cf. Ref. 3 which neglects spatial variations in precursor density); (iii) details of precursor-dynamics coupling to the substrate/chemisorbed layer.

The irreversible cooperative filling (i.e., chemisorption) models considered here are completely characterized by specification of a set of filling rates k_i, which depend on the *local* environment i of the site being filled. To form islands with superlattice spacing, filling is blocked by nearby [e.g., neighboring (NN)] occupied sites, and cooperatively enhanced (relative to the island nucleation rate k_0) by more distant filled sites [e.g., second nearest neighbors (2NN) in one-dimensional (1D) creating double-spaced islands, or next nearest neighbors (NNN) on a two-dimensional (2D) square lattice creating C(2×2) islands]. Note that since island addition rates depend only on the *local* environment, the (individual) islands formed will have compact shape,[4] in contrast to those generated via diffusion-limited aggregation models.[5] When islands of different phase impinge, *permanent domain boundaries* form.

These and other features may be generic for island-forming chemisorption systems at low temperature where kinetic limitations produce small islands[1] [e.g., four-fold degenerate 2×1 O/W(110), three-fold degenerate $\sqrt{3}\times\sqrt{3}$ R 30° CO/Ru(001)]. Only simpler two-fold degenerate models are analyzed here, but the basic behavior and ideas presented have more general applicability.

One can straightforwardly write the master equations for these processes in the form of an infinite hierarchy. Exact solution (via truncation) is possible in one dimension,[6] and some analysis of (double-spaced) island size distributions has been given.[7–9] Approximate truncation techniques have been developed for 2D processes,[10] but simulation combined with analysis of related simplified models will be primarily used here. Here we focus on the scaling of the correlations, island size distribution (particularly a characteristic average linear dimension), with the ratio of (suitable) growth to nucleation rates. In two dimensions, we also consider (growing) island structure, and domain boundary network characterization.

II. DOUBLE-SPACED ISLANDS ON A ONE-DIMENSIONAL LATTICE

Here irreversible filling o→x with NN blocking occurs with rates k_i for sites with i already occupied 2NN. Thus k_0,

 0734-2101/87/041040-05$01.00

k_1, and k_2 correspond to island nucleation, growth, and coalescence, respectively. Double-spaced islands can meet either in phase (..oxoxoooxoxo.., where the center o site fills if $k_2 \neq 0$), or out of phase (..oxoxooxoxo..) creating a permanent domain boundary. Filling continues until *saturation*, where no empty triples remain (and the statistics are independent of $k_2 \neq 0$[7]). Let n_s denote the probability of an island (ooxoxo..oxoxoo) with exactly s filled sites, so $\Sigma_s sn_s = \theta$ is the coverage, and $\Sigma_s n_s = P[\text{xoo}] = P[\text{oox}] = P[\text{oo}] - P[\text{ooo}] = 1 - 2\theta - P[\text{ooo}]$ ($\equiv D$) is the island density. (P denotes probability here.) Thus the average island size (without site weighting), $s_{\text{av}} = \theta/D$, can be determined from local quantities, and reduces to $\theta(1-2\theta)^{-1}$ at saturation.

From a dimensional analysis (cf. Ref. 11), we expect that the characteristic length and time scales are given, in terms of the basic parameter $\alpha = k_1/k_0$, by $\xi_0 = \alpha^{1/2} a$ (a denotes the lattice constant), and $\tau_0 = k_0^{-1}\alpha^{-1/2}$, respectively. This behavior also emerges from simplified lattice[4] and continuum[12] descriptions of the process neglecting fluctuations in island growth. For our 1D model, however, some exact results are available. We have shown previously that the saturation coverage θ^* scales like $1/2 - \theta^* \sim 1/8(2\alpha/\pi)^{-1/2}$, so the corresponding

$$s_{\text{av}}^* = \theta^*(1-2\theta^*)^{-1} \sim 2(2\alpha/\pi)^{1/2},$$

as $\alpha \to \infty$.[7] Figure 1 shows that $\alpha^{1/2}$ scaling of s_{av} also holds for all fixed coverages.

As $\alpha \to \infty$, quantities characterizing the spatial structure on a length scale la should be universal when expressed in terms of $\xi = la/\xi_0$, for fixed $\tau = t/\tau_0$ or $y = \theta/\theta^*$ (cf. Ref. 11). The simplest example involves probabilities $\tilde{P}(l)$ of finding l consecutive sites empty (i.e., an empty segment of the lattice of length $\sim la$). For $l \gtrsim 4$, these satisfy[7]

$$\tilde{P}(l) = \tilde{P}(4)\exp[-(l-4)k_0 t] \sim (1-\theta)e^{-\tau\xi},$$

exhibiting universal exponential decay. Similarly, if $C(l)$ denotes the correlation function for a pair of filled (or empty) sites separated by l lattice vectors, then $C(2l)$ [$C(2l+1)$] should converge to the universal form

$$C^{+(-)}[\xi' = l/s_{\text{av}}, y = \theta/\theta^*] \geq 0 (\leq 0),$$

as $\alpha \to \infty$. Note that $C(0) = \theta - \theta^2$ and $C(1) = -\theta^2$, so

$$C^{+(-)}[\xi' = 0] = y/2 - y^2/4 \ (-y^2/4).$$

For the normalized island size distribution, $P_s = D^{-1}n_s$, one should find that $s_{\text{av}}P_s$ converges to the universal form $P[x = s/s_{\text{av}}, y = \theta/\theta^*]$, normalized in x (for each fixed y), as $\alpha \to \infty$. Monotonically decaying universal $C^{\pm}$ behavior is exhibited by the (readily calculated[13]) $C(l)$ for $\alpha \gtrsim 15$. We also find that $|C^+[\xi]| - |C^-[\xi]| > 0 (=0)$ for $y < 1 (=1)$. Determination of the monomodal P requires much more extensive calculations (since the exact n_s must be determined indirectly),[7,8] and we find much slower convergence to universality (with increasing α).

Finally we note that, for *fixed* (possibly large) α, our previous analyses have demonstrated *asymptotic* exponential [superexponential] decay for the n_s, as $s \to \infty$, if $k_2 \neq 0$[8] [$k_2 = 0$[9]], and *asymptotic* superexponential decay of the $C(l)$.[13] This behavior is nonuniversal (clearly for superexponential decay), and occurs on size or length scales larger than $O(\alpha^{1/2})$.

Next we consider the *angular distribution of the diffracted intensity* $I(q)$ for this system, in the single-scattering approximation. Here $q = \Delta\mathbf{k}\mathbf{a}$, where $\Delta\mathbf{k}$ is the momentum transfer, and $\mathbf{a}$ the lattice vector. Exact behavior [obtained from the $C(l)$],[14] is compared with predictions from the "island size broadening model" (ISBM),[15] which ignores interferences between different islands, as well as with Guinier's formula.[16] The latter accounts for interference by introducing a single (average) island pair distribution function (typically represented via convolution in terms of the corresponding quantity for neighboring islands). We find that the *integral order beam* ($q \approx 0$) intensity,

$$\left[C(0) + 2\sum_{l>0} C(l)\right] \Big/ \theta \sim 4\int_0^\infty d\xi'(C^+ + C^-) \Big/ D$$

trapezoidal rule), effectively vanishes as saturation is approached[14] [where $C^+ \equiv -C^-$, i.e., there is a propensity for cancellation of successive $C(l)$]. Both the ISBM and the Guinier formula *fail* to show this feature.[14] Behavior at the *superlattice beam* ($q \approx \pi$) is of particular interest since Tracy and Blakely[17] conjecture that island interference is not significant there. This would allow determination of the average island size via a simple ISBM algorithm.[15] However, here we find significant interference, and that the Guinier formula again fails.[14] In fact, use of the ISBM algorithm underestimates the average island size (for fixed $y = \theta/\theta^*$, and various α) by a factor which increases to roughly *three* at saturation, $y = 1$.[14]

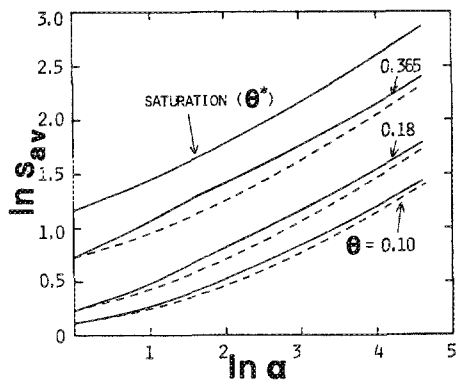

FIG. 1. ln s_{av} vs ln α for 1D double-spaced islands created via filling with multiplicative ($k_0:k_1:k_2 = 1:\alpha:\alpha^2$; solid lines) and quasimultiplicative ($k_0:k_1:k_2 = 1:\alpha:\alpha$; dashed lines) rates. Exact behavior is shown for fixed coverages, and at saturation [where both rate choices coincide, and $s_{\text{av}}^* = \theta^*(1-2\theta^*)^{-1}$]. All slopes approach $\frac{1}{2}$, as $\alpha \to \infty$.

III. C(2×2) ISLANDS ON A SQUARE LATTICE

Here irreversible filling o→x with NN blocking occurs with rates k_i for sites with i already occupied NNN. Thus k_0 corresponds to island nucleation, k_1 to growth, and k_2, k_3, k_4 to growth or coalescence. Individual C(2×2) islands are restricted to one of the two $\sqrt{2}\times\sqrt{2}$ $\pi/4$-rotated square sublattices. Those on the same (different) sublattices are in-phase (out of phase) and coalesce (form a permanent domain boundary) on meeting. Filling continues until saturation, where no empty sites with all four NN empty

remain (and the statistics are independent of $k_4 \neq 0$). Characterization of the island statistics, e.g., average sizes, spanning lengths, and shapes, is more difficult here. It is convenient for us to take a 1D cut through the adlayer, considering the distribution in the number of filled sites in a linear (horizontal or vertical) string (ooxoxo..xoxoo) within a single domain. Specifically we consider the average number (without site weighting) $m_{av} = \theta/(1 - 2\theta - P[\text{ooo}])$ (i.e., the same formula as for 1D s_{av}), but here $P[\text{ooo}] \to 0$ at saturation. There is a direct correspondence between m_{av} and the average cluster spanning length *only* for well separated C(2×2) islands (i.e., low coverages) with an insignificant number of

XOX
OOO
XOX

defects. We shall see that as θ increases a *percolation-type* pattern develops of interpenetrating and nested domains of different phase. Below we discuss, in detail, some specific rate choices.

A. Eden rates, $k_i = \alpha k_0$, for $i \geq 1$ (E)

Here individual islands have asymptotically round Eden structure (on $\sqrt{2} \times \sqrt{2}$ $\pi/4$-rotated sublattice)[4] with an "active or growing zone" width scaling like the radius to the power $p \sim 0.32$ to 0.5.[18] The radius grows, on average, $2\alpha k_0$ lattice vectors per unit time. Simple dimensional analysis determines basic length (ξ_0) and time (τ_0) scales for the $d(\geq 1)$ dimensional hypercubic lattice analog of this process (with lattice constant a). From the nucleation rate of $\Gamma = k_0 a^{-d}$ (dimension $T^{-1}L^{-d}$), and growth rate of $G = 2\alpha k_0 a$ (dimension LT^{-1}), we find that

$$\xi_0 = (G/2\Gamma)^{1/(d+1)} = \alpha^{1/(d+1)} a$$

and

$$\tau_0 = (\Gamma G^d)^{-1/(d+1)} = k_0^{-1} \alpha^{-d/(d+1)}$$

(cf. Refs. 4 and 11). Figure 2(a) shows that $m_{av} \sim \alpha^{\nu}$ where $\nu = \frac{1}{3}$ at saturation (cf. above), but ν is smaller [$= (1-p)/3 \sim \frac{1}{5}$] for fixed coverages $\theta < \frac{1}{2}$. The latter is due to incomplete growth in the active zone (see Ref. 4 for more detail) which fills in at saturation. Figure 2(a) also suggests that, at saturation, $m^*_{av} \sim 1.4\,\theta^*(1-2\theta^*)^{-1}$, so $P^*[\text{ooo}] \sim 0.26(1-2\theta^*)$, as $\alpha \to \infty$.

For large α, we characterize the universal spatial structure on a length scale $\xi = la/\xi_0 = 0(1)$ (for fixed $\tau = t/\tau_0$).[19] Consider Johnson–Mehl plots[12] where circular grains expand at a constant rate G (until impingement) about nuclei generated randomly at a constant rate Γ. At impingement, grain boundaries form which are sections of hyperbolas. These patterns scale like $(G/\Gamma)^{1/3}$. To model C(2×2) island growth with E rates, we randomly assign one of two phases to each grain, and remove boundaries between grains of the same phase. An example of a resulting pattern at saturation is shown in Fig. 3. This description ignores distinct fluctuation behavior on smaller length scales [e.g., C(2×2) domain boundaries are hyperbolic sections modified by fluctuations on a length scale $0(\alpha^p)$], and nonuniversal behavior on a larger length scale (e.g., in the spatial correlations).[8,9,13]

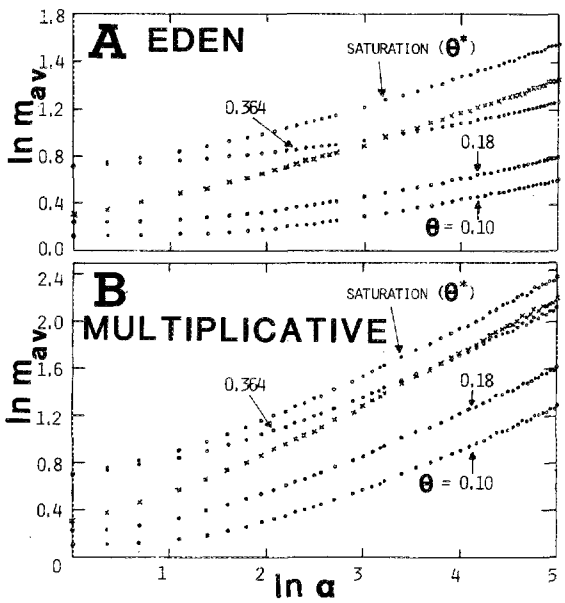

FIG. 2. ln m_{av} vs ln α for C(2×2) islands created via filling with (a) Eden ($k_i/k_0 = \alpha$, for $i \geq 1$) and (b) multiplicative ($k_i \propto \alpha^i$) rates. Each solid point comes from ten computer simulated fillings on a 400×400 periodic lattice. Results for quasimultiplicative rates ($k_0:k_1:k_2:k_3:k_4 = 1:\alpha:\alpha^2:\alpha^2:\alpha^2$) (not shown) deviate only slightly below those for multiplicative rates, and only for moderate α. For A [B], slopes at $\ln\alpha \sim 5$ are roughly 0.31 ± 0.01 [0.46 ± 0.02] at saturation, and 0.20, 0.19, 0.18 ± 0.01 [0.45, 0.43, 0.42 ± 0.02] at $\theta = 0.364$, 0.18, 0.10, respectively. These indicate $\alpha \to \infty$ slopes of $\frac{1}{4}$ [$\frac{1}{2}$] saturation, and $\sim\frac{1}{5}$ [$\frac{1}{2}$] fixed θ. We have also plotted $\ln[\theta^*(1-2\theta^*)^{-1}]$ vs ln α (crosses).

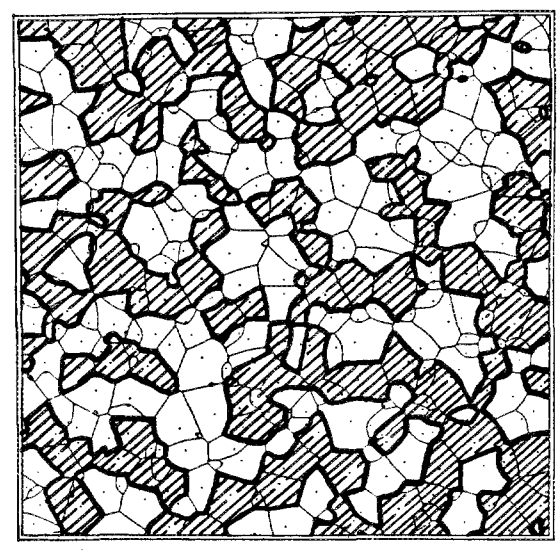

FIG. 3. Adaption of a Johnson–Mehl plot [H. J. Frost and C. V. Thompson, Acta Met. (in press)] to describe the saturation structure for (multi) C(2×2) Eden cluster growth on a length scale $0(\alpha^{1/3})$. Domains of one phase are cross-hatched (all original J–M grain boundaries are shown by light lines, and their nuclei by points). The average grain area is unity on the length scale shown; a unit length corresponds to l_0 lattice vectors where $1.137(2\alpha l_0^{-3})^{2/3} = 1$.

B. (Quasi) multiplicative rates, $k_1 = \alpha k_0$, $k_2 = \alpha^2 k_0$

Here individual C(2×2) islands tend to be diamond shaped (i.e., $\sqrt{2}\times\sqrt{2}$ $\pi/4$-rotated rectangles), for large α, since the rate for completing an edge k_2 is α times the rate for starting a new edge k_1.[4] The probability that an edge of m filled sites is completed before the next layer begins to grow scales like m^2/α,[20] so individual islands retain their diamond shape for sizes up to $m = 0(\alpha^{1/2})$. Here such island edges progress, on average, $\sqrt{2}\ m\ k_1$ lattice vectors per unit time, i.e., they accelerate [m edge sites are available as "nuclei" for the new edge; edge completion occurs sufficiently quickly that k_1 is the growth limiting rate for $m \lesssim 0(\alpha^{1/2})$ and large α].

Determination of island size scaling here is by self-similarity arguments (which could equally be applied for Eden rates). If we adjust the length scale by a factor of λ, the nucleation rate scales like λ^{-2} (for $d = 2$), but the growth rate (for islands whose size is also rescaled by λ) is constant (cf. λ^{-1} scaling for E rates). For the ratio of growth to nucleation rates, which thus scales like $\lambda^{-2}\alpha$, to be constant, we require that $\lambda \sim \alpha^{1/2}$. Corresponding $\alpha^{1/2}$ scaling of the characteristic length has been proposed for single-phase islands formed on lattices with (quasi) multiplicative rates [and follows from a simplified model, which (i) neglects fluctuations in growth and (ii) ignores rapid development of a single larger rectangular island on coalescence of smaller ones].[4] Figure 2(b) shows that, for multiplicative rates, $m_{av} \sim \alpha^{1/2}$ both at saturation, and for fixed coverages [as expected since here the "active zone" has thickness 0(1), so $m_{av}\ a$ corresponds to the characteristic length scale for all θ]. Results for quasimultiplicative rates

$$(k_0{:}k_1{:}k_2{:}k_3{:}k_4 = 1{:}\alpha{:}\alpha^2{:}\alpha^2{:}\alpha^2)$$

are not shown, but deviate only slightly below those for multiplicative rates (and only for moderate α). A consequence of this scaling is that islands tend to retain their diamond shape up to impingement, as reflected in a propensity for "diagonal or staircase" domain boundaries, for large α. Figure 2(b) also suggests that, at saturation, $m^*_{av} \sim \theta^*(1-2\theta^*)^{-1}$, as $\alpha \to \infty$ (diagonal domain boundaries contain no ooo configurations).

C. Comparison and further results

From computer simulations, we have examined the temporal development of the island structure, and determined the spatial pair correlations $C(1)$ for Eden and multiplicative rate choices. For large α, $C(1)$ display universality on a length scale $0(m_{av}a)$. In Fig. 4, we have compared saturation states (for the same coverage). Note the similarity between Fig. 4(a) (Eden rates) and Fig. 3, and observe the propensity for diagonal domain boundaries in Fig. 4(b) (multiplicative rates). The corresponding integral order beam diffracted intensities diminish dramatically at saturation for both rate choices [a consequence of $C(1)$ universality and the saturation identity $C^{++} \equiv -C^{--}$, naturally extending the 1D definition of $C^{\pm}$]. Superlattice beam shapes are quite different for the two rate choices (with the same m_{av}). In a future communication, we shall detail the relationship between superlattice beam half-widths and m_{av}^{-1} or similar quasi-one-dimensional quantities.

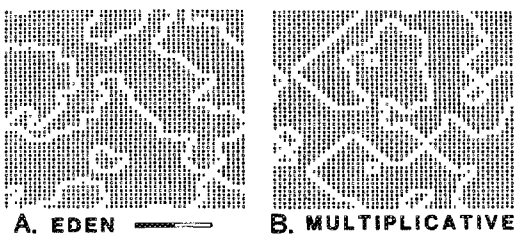

FIG. 4. Comparison of saturation states for (a) $\alpha = 200$ Eden, and (b) $\alpha = 30$ multiplicative rates, with the same $\theta^* \sim 0.4452$ (X and Y denote filled sites in domains of different phase; 0 denoting empty sites are left out at the domain boundaries for contrast). The length scale shown for Eden rates corresponds to that in Fig. 3 (here $l_0 = 7.86$).

IV. SUMMARY AND EXTENSIONS

Our results elucidate the structure of nonequilibrium islands and domain boundaries formed in a class of models for irreversible cooperative chemisorption, focusing on the scaling of the characteristic length with the ratio of (suitable) growth to nucleation rates α. Modified grain growth models help to elucidate the large α behavior (for Eden rates). They also indicate that the saturation state is close to percolation (cf. Figs. 3 and 4).[19] We have also explained the diffracted intensity diminution (as saturation is approached) in the integral order beams, and observed significant interference at the superlattice beams.

ACKNOWLEDGMENTS

Ames Laboratory is operated for the U. S. Department of Energy by Iowa State University under Contract No. W-7405-Eng-82. This work was supported by the Office of Basic Energy Sciences.

[1] M. G. Lagally, G.-C. Wang, and T.-M. Lu, in CRC Crit. Rev. Solid State Mater. Sci. 7, 233 (1978).
[2] E. S. Hood, B. H. Toby, and W. H. Weinberg, Phys. Rev. Lett. **55**, 2437 (1985).
[3] N. O. Wolf, D. R. Burgess, and D. K. Hoffman, Surf. Sci. **100**, 453 (1980).
[4] J. W. Evans, J. A. Bartz, and D. E. Sanders, Phys. Rev. A **34**, 1434 (1986).
[5] *Kinetics of Clustering and Aggregation*, edited by F. Family and D. P. Landau (North-Holland, Amsterdam, 1984).
[6] E. A. Boucher, J. Chem. Soc. Faraday Trans. **69**, 1839 (1973); J. J. Gonzalez, P. C. Hemmer, and J. S. Hoye, Chem. Phys **3**, 228 (1974); N. O. Wolf, J. W. Evans, and D. K. Hoffman, J. Math. Phys. **25**, 2519 (1984).
[7] J. W. Evans and D. R. Burgess, J. Chem. Phys. **79**, 5023 (1983).
[8] R. S. Nord, D. K. Hoffman, and J. W. Evans, Phys. Rev. A **31**, 3820 (1985), see Sec. V.
[9] J. W. Evans and R. S. Nord, Phys. Rev. A **31**, 3831 (1985), see Sec. VI.
[10] J. W. Evans, D. R. Burgess, and D. K. Hoffman, J. Chem. Phys. **79**, 5011 (1983).
[11] J. D. Axe and Y. Yamada, Phys. Rev. Lett. B **34**, 1599 (1986).
[12] W. A. Johnson and R. F. Mehl, Trans. AIME **135**, 416 (1939).
[13] J. W. Evans, D. R. Burgess, and D. K. Hoffman, J. Math. Phys. **25**, 3051 (1984).

[14]J. W. Evans and R. S. Nord, Phys. Rev. B. **35**, 6004 (1987).
[15]M. G. Lagally, T.-M. Lu, and G.-C. Wang, in *Chemistry and Physics of Solid Surfaces*, edited by R. Vaneslow (CRC, Boca Raton, FL, 1979), Vol. II.
[16]A. Guinier, *X-ray Diffraction* (Freeman, San Francisco, 1983), Chap. 2; J. E. Houston and R. C. Park, Surf. Sci. **21**, 209 (1970).
[17]J. C. Tracy and J. M. Blakely, in *The Structure and Chemistry of Solid Surfaces*, edited by G. A. Somorjai (Wiley, New York, 1969), Vol. II, Paper No. 65.
[18]M. Plischke and Z. Racz, Phys. Rev. A **32**, 2825 (1985); P. Freche, D. Stauffer, and H. E. Stanley, J. Phys. A **18**, L1163 (1985). Here we *neglect* effects of lattice anisotropy.
[19]J. W. Evans (in preparation); C(2×2) domains cannot percolate at saturation since domains of *both* phases would have to simultaneously percolate. However, the (percolative) correlation length can become large if the system is "close to" percolating. This is expected at least for $\alpha \to \infty$ Eden rates: here create a "random" lattice by connecting nuclei of neighboring J–M grains (neglecting lenses). The average coordination number $\bar{z}$ is 6 by Euler's theorem; the site percolation threshold p_s is probably close to $\frac{1}{2}$ (cf. a triangular lattice with $z = 6$ and $p_s = \frac{1}{2}$). Here, theoretically $p_s \geqslant \frac{1}{2}$ (so $p = \frac{1}{2}$ cannot be panchromatic for two-color percolation).
[20]For most adsorption events, the ratio of (total) probabilities of edge growth to nucleation of the next layer is $0(m/\alpha)$, and growth must occur $0(m)$ times for edge completion.